Proceedings World Geothermal Congress 2020+1
Reykjavik, Iceland, April - October 2021

Adding Value on the Inverse Problem Solution by Modeling the Tipper Vector and the Total Magnetic Field

Dagoberto Herrera

ICE, IC, CSRG, P.O. Box. 1032-1000 SJ. CR.

dherrere@ice.go.cr

Keywords: Tipper vector, inverse modelling, Las Pailas, geothermal field.

ABSTRACT

In lithostratigraphic terms, the volcanic environments are complex. Prior information is required to facilitate the solution of the inverse problem. It is necessary to evaluate hypotheses according to existing geological and geophysical data. However, aspects such as EM field distortions, conductive faults, or deep electrical conductors, for example, could increase its ambiguity. The magnetotelluric interpretation suits well for testing these hypotheses. With tipper's magnitude and strike, together with a potential method, is possible, to locate and identify conductive and non-conductive structures, that helps to recognize traces and structural scenarios. The case of the geothermal resources of Las Pailas, phase II, is analyzed, with the results of ground magnetics exploration, and tipper vector data from previous MT electromagnetic campaigns. These data fed back, support a simplified conceptual model of the geothermal field during its development. A correlation was observed in a specific geological environment showing possible structural and lithological relations through the use of intuitive geophysical tools, like the total magnetic field map, filtered, and a classical approach by MT exploration, evaluating the tipper.

1. INTRODUCTION

The main issue in doing the inverse modelling is to approximate the real geology by a simple model, trying to determinate model parameters out of a subset of data, by inverse modelling them. The principal assumption is that the physical properties of the medium are known. We usually need to answer to; is there a solution? Is it unique? Is the solution stable? There must be a solution for certainty, as within geoscience´s subjects are to study the geological phenomena of earth interior. The positive answer to all of these questions might constitute a well-posed problem from the geophysical point of view. However, the majority of the geophysical problems are ill-posed. The principal assumption is that the physical properties of the medium are known. The best approach goes through the integration of independent variables.

Two methods became available for comparing and integrating: ground magnetics total field and the Tipper vector, that together add value and reduce ambiguity to working models, and its discrepancies. As it happens for instance with, the non-uniqueness of potential fields problems, which results in the introduction of constraints, in the form of simplification of the geometry, limits to size or depth, range limits on susceptibility, or whatever other parameter is justified in the context of what is known or what can be inferred about geological environment. With the use of independent variables like induction arrows, these limits can be established, at least it most plausible choice. The figures were placed at the end of the document to preserve an easily visible scale.

2. BACKGROUND INFORMATION

With the operation of the Pailas II powerhouse, the geothermal installed capacity in costa Rica reached around 15% of the total energy consumed in the country. Though it began since 196, it was not but until 2003 that the first 5 wells were drilled on the western flank of Rincon de La Vieja volcano. Two geothermal power plants have been installed, Unit I (41.5 Mwe) with 21 wells and Unit II (55 Mwe) with 22 wells. In average it was drilled down to 2200 m. In general, the geothermal resource lies between 100 and 800 m below sea level, with temperatures that range from 205°C-250°C. It is a liquid dominant type reservoir, with a neutral pH (7,48-7.85), high TDS (12165-13010 ppm), and with low non-condensable gases in steam (0.88 % w/w).

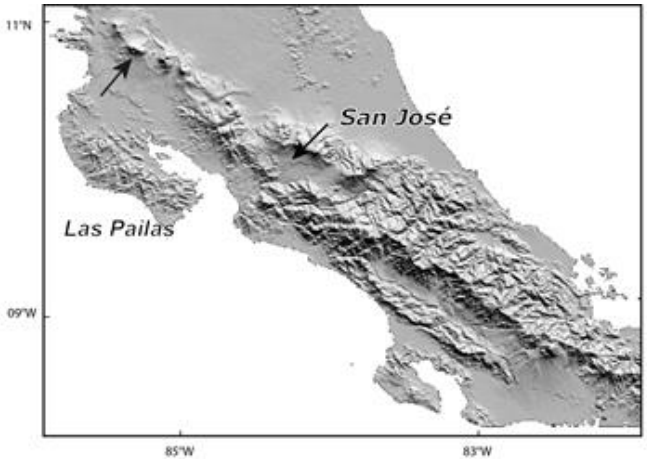

Figure 1 Location of Las Pailas field. SRTM image (NASA, Shuttle Radar Topography Mission released of 2015).

2.1 Geological setting

The Guanacaste volcanic range at the north of the country was formed about 0.6 Ma and comprised four stratovolcano complexes (1500-2000 m high). Being Rincon de la Vieja-Santa María and Miravalles two of them. Miravalles is the highest in the zone and is related to a 15 km wide caldera with the latest activity <0.28 Ma. Rincón de la Vieja instead is the largest volcano, with an estimated volume of 130 km3. (Carr, 1984) It is a complex andesitic stratovolcano with nine coalescing pyroclastic cones spread over an axis 8 km long. The earlier activity was a Plinian eruption 3,500 years ago. It has been characterized by phreatic/phreatic-magmatic eruptions from the active crater.

Las Pailas geothermal field lies at a flank of the latter, about 10km west of Alfredo Mainieri geothermal field (Fig 1) at Miravalles volcano. Its structure is well known from several geophysical methods (gravimetry, magnetics and MT) and 32 deep production wells. The lateral extent was mapped out by regional MT campaigns. Most of the area is covered by thick andesite's sequences, basalts and pyroclasts, whereas at the center consists of lahars and avalanches that came from the volcanic edifice. Toward the west, there are conglomerates deposits. A characteristic of this area is the development of several lava domes, e.g., caldera structure known as Cañas Dulces, which are dacitic. This caldera partially limits the geothermal field. The caldera structure itself shows lavas and pyroclastic flows of dacitic composition.

Geothermal activity has been related to the evolution of caldera structures as well as with a structural scenario mostly controlled by the subduction mechanics. The geothermal field is located inside a concentric caldera and is mainly composed of andesitic-basalt to rhyolitic sequences together with pyroclastic and effusive events. To the west and south of the geothermal field, dacitic lavas and ignimbrite deposits have been crossed. Close to the caldera border high-temperature alteration mineralogy deepens, and the low-temperature smectite zone becomes thicker.

2.1.1 Structural setting

One of the foremost tectonic structure or family of structures, at the top right corner of the figures 2-6, has an elongated NNW-SE strike, of very long distance, parallel to the trench path, and thermal manifestations. Secondary oblique lineations to them are considered to be secondary stress-related Riedel faults (WJEC 2013). However, the hydrogeology is a complex phenomenon. The area is characterized by a caldera structure, intercepted by NW-SE, NE-SW faults, and other fault groups; with an E-W, N-S strike. Lastly, there is another NNW-SSE system toward the center of the field. Some of them have been drilled and suggested permeability expectations to Las Pailas phase II at the east.

Another important element is the caprock. It was defined by clay types zonation, quartz anomalies, epidote and loss zones, which resulted in a general observation: the caprock becomes shallower and thinner toward the volcano structure and deepens and thicker to the south, southwest, and west showing a lower temperature gradient as well. The geometry of the caprock mimics the quartz zone, and the illite/smectite zone (Hakanson et al., 2015). The geometry of the resource is represented by the caprock; therefore, it is a rather important element of the modelling. From figures 2 to 5, the faults are in dark red. The heat source is considered to the north, outside the area.

3. BACKGROUND OF METHODS

3.1 Tipper anomalies

One way to represent the soil resistivity structure is through the graphical presentation of induction arrows (tipper, defined in the sense of Wiese-Parkinson matrix). They represent the conductivity structure of subsurface, controlled or determined typically – in geothermal systems- by secondary alteration at different depths. The vectors transform or tips horizontal magnetic fields into vertical ones (Vozof 1972). In matrix notation:

$$H_z = [W]\mathbf{H_T}$$

$$[\boldsymbol{W}] = [\boldsymbol{W_{zx}}\,\boldsymbol{W_{zy}}] \qquad \boldsymbol{H_T} = \begin{bmatrix} \boldsymbol{H_x} \\ \boldsymbol{H_y} \end{bmatrix}$$

H_z is expressed as a linear combination of horizontal magnetic field components, H_x and H_y given by $Hz = W_{zx}H_x + W_{zy}H_y$. The tipper then is sensitive to current distribution that in excess occurred over the horizontal resistivity variation (galvanic and inductive), the vertical magnetic fields thus generated and its effect, as the lateral conductivity gradients are used to recognize lateral variations (Simpson and Bahr). The vectors point toward anomalous current concentrations following Parkinson convention (Parkinson 1959).

Therefore, for 1 D earth, there is not any induced current vertically, hence the Wiese-Parkinson matrix is null. However, for 2 D (associated with E-polarizations) using a rotation of its coordinate system, H_x can be minimized, and W_{zx} diminished, while W_{zy} increase or maximizes. Given the condition, the X-axis is now parallel to the strike, which is also known as the tipper strike and will follow the resistivity gradient (black roses in figures 2 and 4).

The electric strike often correlates with the main resistivity distribution, also expressed as the rock deformation patterns, e.g., faulting shear zones (its intensity of alteration). At higher periods the tipper vectors point away from a conductive zone (Berdichevsky and Dimitriev 2002). These results should be consistent with the resistivity modelling anomalies. The principal tipper direction is not ambiguous for a perfect 2D earth, as it always points toward the resistive side of the contact that induces the vertical magnetic field component. It may represent a clear picture of the strike direction, and at low frequencies, it is considered that the magnetic field tends to become free of shallow distortions.

The presence of high-temperature geothermal areas may alter geoelectric strike direction at different depths. Moreover, Eystensson (2010) and Karlsdottir et al., (2012) in Khyzhnyak (2014), after comparing strike directions from Krafla and Námafjall geothermal

areas, conclude that Tipper strike follows zones of anomalous resistivity rather than dominant geological strike. This implies that the analysis of geoelectric strike direction in MT measurements and its interpretation and application should be observed more carefully.

Induction arrows for both real and imaginary parts are derived from the tipper, the plotted real component arrows (red color in figure 2) are considered intuitively easier to understand, and often points away from regions of enhanced conductivity, while the imaginary part will change sign where real parts are maximal. Induction arrows also have been used for dimensionality analysis, the real part of induction vectors is orthogonal to geoelectric strike, and are being used to solve the 90 ° ambiguity obtained from the tensor solution. As mentioned, the real induction arrows should point away from good conductors in a two-dimensional setting. The arrows may hint at a conductive anomaly body beneath the MT sites. From the behavior of the arrows, we can conclude that a 2-D interpretation will be meaningful for the data.

3.1 Magnetic anomalies

It is a passive method base on susceptibilities changes. Simple and of low cost. It helps with the geological mapping of units, faults, fractures, depth to basement and its geometry as a consequence. It is useful for checking lateral variations but should have a careful geological control.

Interpretation of magnetic anomalies requires the reduction of a normal magnetic field from any disturbing regional effect. Magnetics anomalies from ground magnetic surveys allow a better understanding of fine structures from shallow partially demagnetized rocks, lying within the resistivity boundary previously defined.

Besides using the entire field reduced to pole, an attempt was made with a first derivative, trying to sharpen the edges of anomalies and to enhance shallow features. The vertical derivative map should be much more responsive to local influences than to broad or regional effects and therefore tends to give sharper picture than the map of the total field intensity. Thus, the smaller anomalies are more readily apparent in the area of strong regional disturbances. The first vertical derivative is used to delineate high-frequency features more clearly where they are shadowed by large-amplitude, low-frequency anomalies.

4. RESULTS

Of the 213 MT soundings, 184 included the full tipper, sampled to have 83 frequencies going from 0.0005 to 899 Hz, but only twenty-eight out of 70 stations were reviewed for tipper strike analysis, bounded to the smaller area here shown, where the development of what is known as Las Pailas II was considered.

Mean tipper strike was computed for two frequency bands shown in Fig. 2 and 4 from 100-10 Hz, and 10-0.1 Hz. In the frequency band of 100–10 Hz, the mean strike is northwest or east–northeast (Fig. 2). while in the range of 10-0.1 Hz frequency bands are even more constrained, less scattered. It can be seen through toward the N and NE, how they scatter out; at the center, and right corner of the area, with noteworthy discrepancies, in terms of wider frequencies distribution. There is a rapid change in the direction of both real and imaginary, components which could be evidence of a 3D anomaly of the sector.

The change of strike suggests that there may be some effect due to the low intensity of the signal, and by some 3D local effect.

It is also possible to observe, how the NW-SE fractures, very large in extension, are emulated by the tipper strike, especially for what Pailas II concern.

According to the field layout of each MT site, the E_x component is in the north-south direction. We did not rotate the data according to due to the scattered strike directions profiles used. Instead, the data were later rotated. After the rotation, the *XY* component corresponds to the *TE* polarization mode in which electric currents flow along the faults, while the *YX* component corresponds to the *TM* mode with electric currents flowing normally to the faults.

Induction vectors were calculated with the convention of pointing away from conductors, the length is small, and some of them at the N and NE are not symmetric, e.g., the shallower components have smaller manifestations horizontally, getting closer to 1D condition with an average resistivity of 10 ohms, which stands for a skin depth of 500 m. For the 100 Hz scenario again, the greatest discrepancies occur to the north and northeast. The mean strike of the induction arrows is generally perpendicular (the real component in red) to these major faults though.

The magnetic map was obtained from 229 stations in total, arranged in 5 profiles, sampled with an average of 46 sites per profile. The total magnetic field thus obtained was reduced to pole.

An ample negative magnetic anomaly occurs over the northern part, at the center and to the right corner of the area. Mainly in blue color. All of negative residuals anomalies occur over surficial thermally altered zones. Incidentally, especially the one at the center. Furthermore, there is this large amplitude and low-frequency anomaly, in red color that controls much of the area to the south. For this one, in particular, it was tried to reduce its effect by a first-order derivative (Fig. 6), but it was hard to clean the map to something more clearly defined with sharp edges. However in the first derivative map, some anomalies were enhanced, like the blue one at the center, that looks longer, while the positive anomaly, recedes and decreases its amplitude. Somehow, wells that were drilled all its trajectory over this positive anomaly resulted in a diminished productivity index.

4. CONCLUSION

As was pointed out previously, the clay cap is deepening and getting thicker to the south as well as it becomes shallower and thinner toward the flanks of the volcano, which very likely is constraining the tipper strike. Furthermore to the N, NE, characteristically occur the transition of smectite, smectite-illite, illite, in thin packages, since they occur as huge levels, that may be intervening in the dispersion of tippers strike, and small magnitude of the induction arrows. For the 10 Hz scenario, the major

scattering of induction arrows happens to the north at a negative magnetic anomaly. There, are the most evident fumaroles of the area.

The nearest wells to this area (white traces), at the NE, showed low permeability, a dike of unknown nature, and high temperatures. The tipper strike and the induction arrows are representing structural conditions of the reservoir there. The phenomenon gets complicated if we consider other tectonic constraints such as the caldera borders.

In the classical approach, the strike draws the NE strike faults; the limits of the reservoir also do.

The magnetic anomalies, on the other hand, correspond to a sort of permeability barrier toward well PGP-10,PGP-9 and perhaps PGP-6. PGP-5 demonstrates a permeability boundary constituted with very thick smectite zone and a very deep Illite occurrence for the S and SW of the area. It may be related to contact between hydrothermally demagnetized and magnetized rocks strike, along a structural lineament that suggests a current hydrothermal activity. Locally confined intense magnetic anomalies on the north are interpreted as dikes with high magnetization.

Magnetic anomalies closely correlate with heat-flux data and surface hydrothermal manifestations and indicate that at the N and NW are characterized by a large, well-developed and active, hydrothermal field. The total magnetic field map shows strong signals that locally are not quite well explained to the south.

The wells were the vectors shows greater scattering a the center of the area coincides with a radon anomaly.

REFERENCES

Berdichevsky, M.N. and Dmitriev, V.I. (2002), "Magnetotellurics in the context of the theory of ill-posed problems," Society of Exploration Geophysicists, 215 pp.

Cumming, William; Di Pippo, Ronald; Duffield, Wendell; Horne, Roland; Truesdell, Alfred. Report of the Twentieth Meeting of the Miravalles Geothermal Project Advisory Panel. Miravalles Geothermal Field 20th Advisory Consultant Panel Meeting. Costa Rica (In Spanish). (March 2005).

Fiona, S., Karsten B. (2005): Practical Mangetotellurics, Cambridge University Press, United Kingdom, 246 pp.

Gylfi Páll Hersir, Knútur.: 3D inversion of magnetotelluric (MT) resistivity data from Krýsuvík high temperature geothermal area in SW Iceland Proceedings, Thirty-Eighth Workshop on Geothermal Reservoir Engineering Stanford University, Stanford, Cal, February 11-13, (2013).

Geoscience Energy. Jeotermal Radon Gazı Ölçümü LasPailas, http://www.gseenergy.com/blog/blog/jeotermal-radon-gazi-olcumu-las-pailas.(2007).

Hakanson, Edward C; Ramirez Salazar, Ronald; Mora Protti, Oscar; Gálvez Orellana, María. Update of the Geologic Model at the Las Pailas Geothermal Field to the East of Unit 1 Proceedings World Geothermal Congress Melbourne, Australia. (2015).

H.L. Lam, F.W. Jones, R.D. Hibbs. The Response of Perturbation and Induction Arrows to a Three-Dimensional buried anomaly. Geophysics, Vol- 47. No 1. (January 1982). P.51-59.

Khyzhnyak Mykola. Geoelectric Strike and its Application in Magnetotellurics. BSc thesis. School of Engineering and the Natural Sciences University of Iceland. (2014).

Osvaldo Vallejos, R.: The Miravalles Geothermal System, Costa Rica. Short Course V on Conceptual Modelling of Geothermal Systems. UNU-GTP and LaGeo, El Salvador. February 24 – March 2. (2013).

Sánchez Rivera, Eddy; Vallejos Ruiz, Osvaldo and González Vargas, Carlos: Maintenance of the Production in the Miravalles Geothermal Field, Costa Rica: New Productive Zones. Proceedings World Geothermal Congress 2010. Bali, Indonesia.

Vega Zúñiga, Eduardo; Chavarría Rojas, Leyner; Barrantes Víquez, Manuel; Molina Zúñiga, Fernando; Hakanson, Edward C., and Mora Protti, Oscar. Geologic Model of The Miravalles Geothermal Field, Costa Rica. Proceedings World Geothermal Congress 2010. Bali, Indonesia. (2010).

Tassi, Franco; Vaselli, Orlando; Bini, Giulio; Capecchiacci, Francesco; Maatern de Moor, J; Pecoraino, Giovannella, Pecoraino; Venturi, Stefania. The Geothermal Resource in the Guanacaste Region (Costa Rica): New Hints from the Geochemistry of Naturally Discharging Fluids. Earth Sci., 05 June 2018. https://doi.org/10.3389/feart.2018.00069.

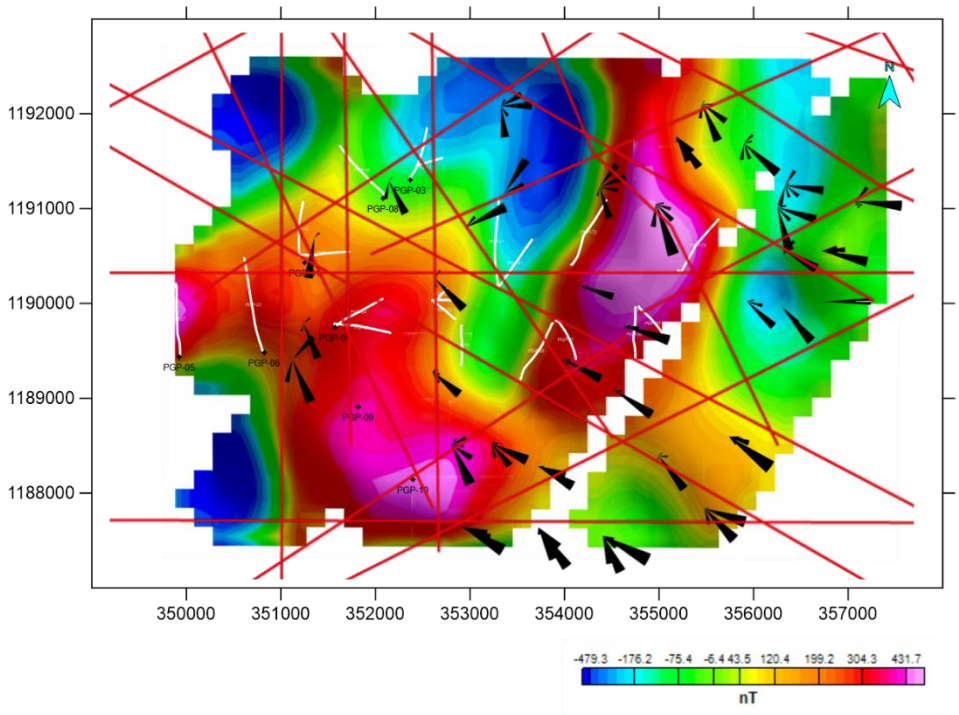

Figure 2: Tipper strike semi-roses in black, faults in red, some wells for reference in white, lastly the total magnetic field signal in the background, the parallelism of the tipper strike is evident. Look for the zones where the trend breaks. Tippers strike in the range of 10 Hz.

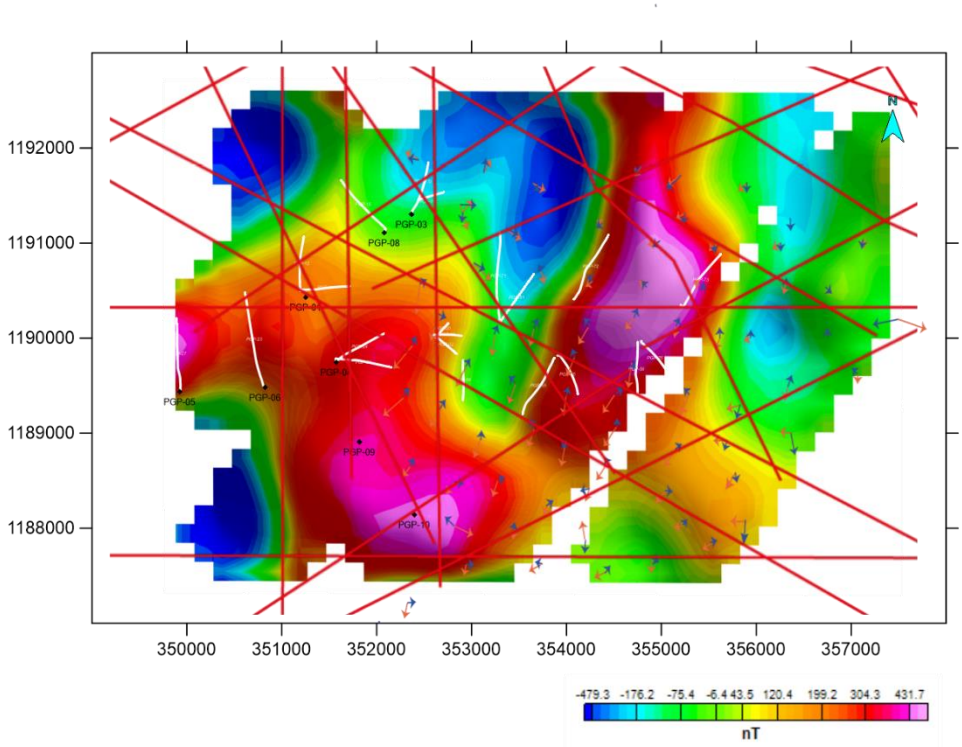

Figure 3: Induction arrows in red (real component) and blue (imaginary component), faults in red, some wells for reference in white, lastly the total magnetic field signal in the background, the general trend is that the real part of induction arrows are perpendicular to the tipper strike. Look for the zones where the trend breaks. Induction arrows in the range of 10 Hz.

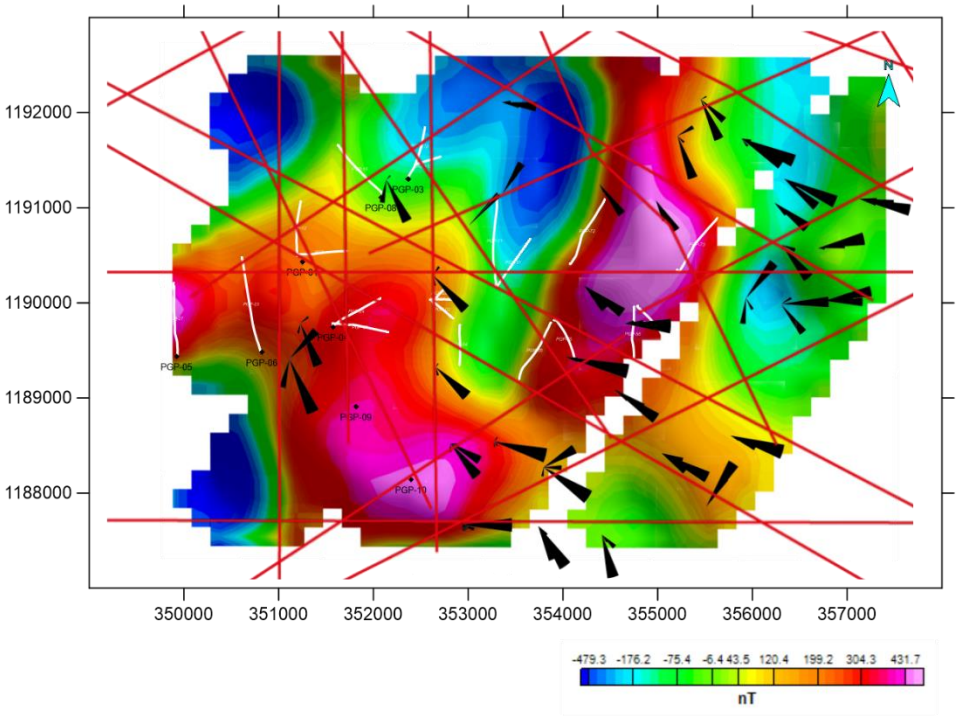

Figure 4: Tipper strike semi-roses in black, faults in red, some wells for reference in white, lastly the total magnetic field signal in the background, the parallelism of the tipper strike is evident. Look for the zones where the trend breaks. Tippers strike in the range of 100 Hz.

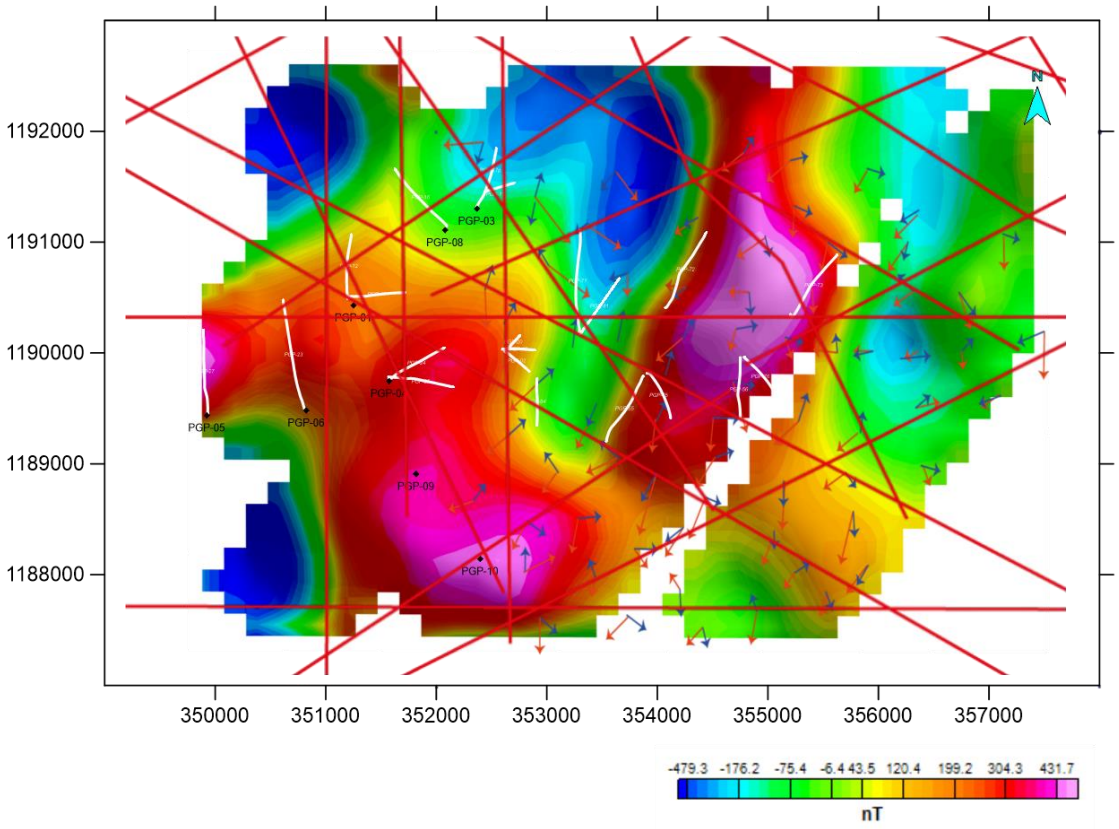

Figure 5: Induction arrows in red (real component) and blue (imaginary component), faults in red, some wells for reference in white, lastly the total magnetic field signal in the background, the general trend is that the real part of induction arrow is perpendicular to the tipper strike. Look for the zones where the trend breaks. Induction arrows in the range of 100 Hz.

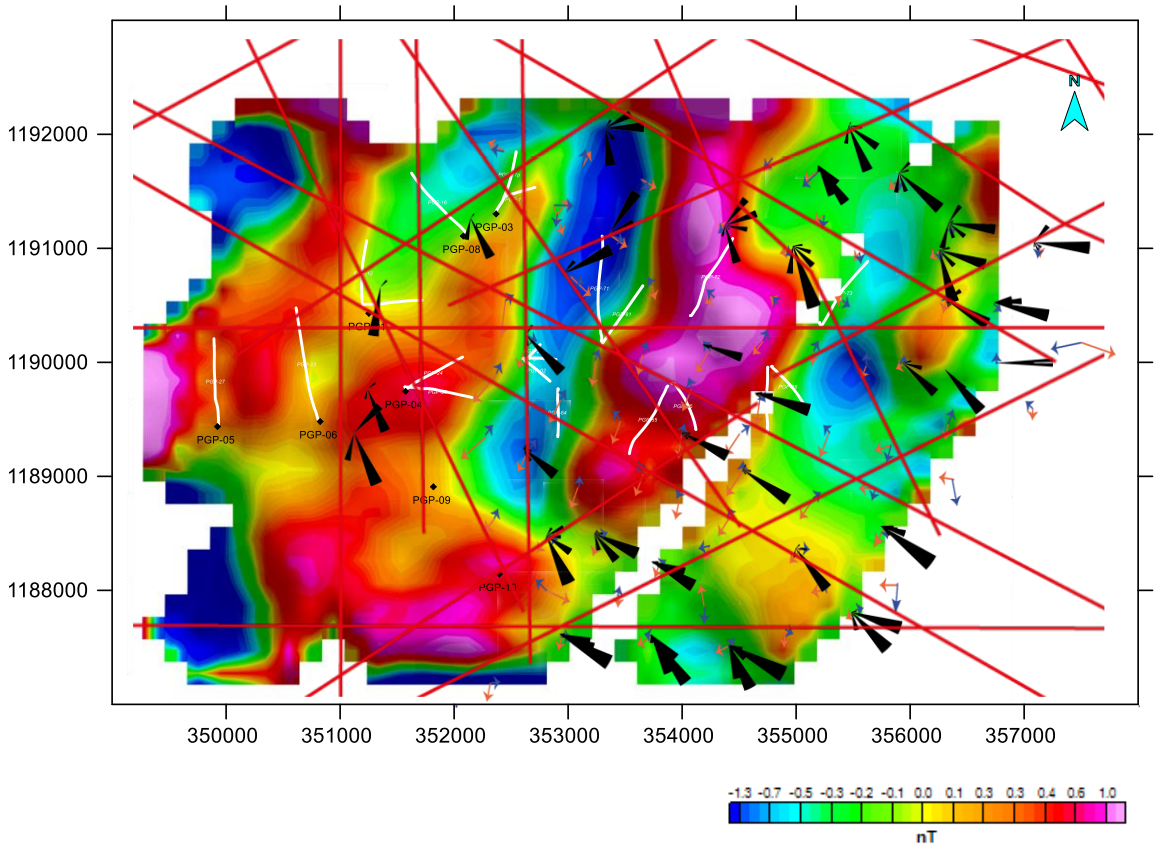

Figure 6: Induction arrows in red (real component) and blue (imaginary component), tipper strike in black, faults in red, some wells for reference in white and black dots, lastly the first derivative of the magnetic total field signal in the background, the general trend is that the real part of induction arrow is perpendicular to the tipper strike. Look for the zones where the trend breaks close or within the enhanced blue zones at the center. A comparison made for tippers strikes in the range of 10 Hz.